

## Re-examination of the possible tidal stream in front of the LMC

Rodrigo A. Ibata<sup>1</sup>, Geraint F. Lewis<sup>2</sup> & Jean-Philippe Beaulieu<sup>3</sup>

### ABSTRACT

It has recently been suggested that the stars in a vertical extension of the red clump feature seen in LMC color-magnitude diagrams could belong to a tidal stream of material located in front of that galaxy. If this claim is correct, this foreground concentration of stars could contribute significantly to the rate of gravitational microlensing events observed in the LMC microlensing experiments. Here we present radial velocity measurements of stars in this so-called “vertical red clump” (VRC) population. The observed stellar sample, it transpires, has typical LMC kinematics. It is shown that it is improbable that an intervening tidal stream should have the same distribution of radial velocities as the LMC, which is consistent with an earlier study that showed that the VRC feature is more likely a young stellar population in the main body of that galaxy. However, the kinematic data do not discriminate against the possibility that the VRC is an LMC halo population.

*Subject headings:* galaxies: individual (Large Magellanic Cloud) — Galaxy: halo

---

<sup>1</sup>European Southern Observatory Karl Schwarzschild Straße 2, D-85748 Garching bei München, Germany  
Electronic mail: ribata@eso.org

<sup>2</sup>Fellow of the Pacific Institute for Mathematical Sciences 1998-1999,  
Dept. of Physics and Astronomy, University of Victoria, Victoria, B.C., Canada &  
Astronomy Dept., University of Washington, Seattle WA, U.S.A.  
Electronic mail: gfl@uvastro.phys.uvic.ca  
Electronic mail: gfl@astro.washington.edu

<sup>3</sup>Kapteyn Astronomical Institute 9700 AV Groningen, The Netherlands  
Electronic mail: beaulieu@astro.rug.nl

## 1. Introduction

Approximately 16 microlensing events have been found by the MACHO collaboration (e.g. Alcock *et al.* 1997a) in their 4 year study of microlensing towards the LMC (Cook 1998). Since this event rate exceeds the microlensing event rate expected from standard models of the Galactic disk, thick disk and spheroid components, they conclude that a significant fraction — most likely half — of the mass in the Milky Way is to be found in massive baryonic compact objects which are distributed in an extended halo around the Galaxy. The combined EROS and MACHO databases rule out the possibility that the lensing masses are sub-stellar (in the range  $3.5 \times 10^{-7} M_{\odot} < M < 4.5 \times 10^{-5} M_{\odot}$ , Alcock *et al.* 1998); and the most probable mass appears to be in the regime typical of stars (Alcock *et al.* 1997a).

However, several studies have proposed alternatives to the conclusion that the lensing masses are genuine halo objects. For instance, some of them could belong to normal stellar populations in the LMC itself (Sahu 1994, Alcock *et al.* 1997b), though it appears that this possibility alone cannot account for the observed event rate. Alternatively, either the lenses or the sources could belong to a tidal structure either in front of, or behind, the LMC (Zhao 1998a); such a structure could be a disrupted remnant of a former dwarf satellite galaxy or a tidally stripped part of the LMC itself. It is possible that the combination of such “normal” microlensing events could account for the total observed event rate. If so, the case that baryonic dark matter has been detected in the LMC microlensing experiments would be substantially weakened. Observational evidence for these objections was presented in 1997, when Zaritsky & Lin suggested that a vertical feature in the color-magnitude diagram seen directly above the LMC “red clump” could be due to an intervening population about 20 kpc in front of the LMC. The color-magnitude diagram of a central LMC field is shown in Figure 1; we draw attention to the region in color-magnitude parameter space of the Zaritsky & Lin “vertical red clump” (VRC) feature by surrounding it with a box. The boxed region covers the color-magnitude range  $0.49 < V - R < 0.6$ ,  $17.85 < V < 18.7$ ; the color limits were chosen visually to encompass the feature of interest, while the magnitude limits help us select possible foreground red clump stars between  $\sim 10$  kpc to  $\sim 25$  kpc in front of the LMC. Beaulieu & Sackett (1998) confirmed photometrically the existence of the VRC, but showed that the CMD-structure of the feature is consistent with being a young stellar population within the LMC itself. The observed characteristics and densities in the VRC are precisely reproduced with a simple model and a few basic assumptions: stellar evolution models from Bertelli *et al.* (1994), an LMC distance modulus of 18.3 mag, an IMF with a slope of -2.8 and a constant star formation history over the last gigayear.

We set out to perform a complementary investigation of the nature of these VRC stars,

using radial velocity measurements to determine the kinematics of the population, as this provides a direct test of the competing hypotheses that does not rely on any modeling or stellar evolution calculation. In particular, any discrepancy in the kinematic properties of the VRC population with respect to the LMC would provide a clear indication that the line of sight to the LMC contains some additional population that is distinct from the LMC.

## 2. Spectroscopic observations

On May 3rd, 1998, we used the ARGUS bench-mounted multi-fiber spectrograph at the 4m Cerro Tololo Interamerican Observatory (CTIO) to observe a field in the central regions of the LMC. The KPGLD3 grating was used in conjunction with the LORAL3k CCD detector to give spectra with  $1.1\text{\AA}/\text{pixel}$  resolution, covering the range between  $4000\text{\AA}$  and  $7500\text{\AA}$ .

With ARGUS, 24 fibers can be placed over a circular field of approximately  $40'$  in diameter, though the fiber positioners are not allowed to touch or cross over. Each positioner also has a secondary fiber with which allows the sky spectrum to be probed close to the target of interest. Unfortunately, the region where our CCD photometry had accurately calibrated astrometry was quite small (approximately  $6' \times 6'$ ), which meant that it was not possible to place all fibers on objects of interest. We exposed two fiber setups, observing 24 stars that lie within the boxed region of Figures 1 and 2, plus 16 stars that lie outside that region. The objects for which ARGUS spectra were obtained are marked with a large dot in the color-magnitude diagram in Figure 2. Each fiber setup was exposed for 3600 sec, giving  $S/N \sim 10$  for the faintest stars observed. The sky spectrum, constructed by performing a median of the sky-fiber spectra, was subtracted from the (fiber-response corrected) stellar spectra. Judging by the size of remaining emission lines in the spectra, the sky subtraction is accurate to  $\sim 5\%$ . Details of the data-reduction techniques used with this instrumental setup can be found in Suntzeff *et al.* (1993).

The resulting velocity data are listed in Table 1, which contains accurate coordinates, photometry, Tonry-Davis cross-correlation  $R$  values (Tonry & Davis 1979), heliocentric radial velocities and radial velocity uncertainties for 40 stars. The radial velocity uncertainties in Table 1 are derived from the cross-correlation peak fit of the survey stars with the template (the G8 III star HR6468 — which gave the best cross-correlation  $R$  values of all the observed templates), and are therefore only indicative.

In the top panel of Figure 3, we show the velocity distribution of the 24 spectroscopically observed stars that lie inside the boxed region of Figures 1 and 2. The maximum-likelihood

Gaussian fit to the velocity distribution of this sample is found to have a mean of  $267 \pm 5 \text{ km s}^{-1}$ , and a velocity dispersion of  $25 \pm 4 \text{ km s}^{-1}$ . The bottom panel displays the velocity distribution of the 16 remaining stars. The Gaussian function fit to these stars has a mean of  $270 \pm 4 \text{ km s}^{-1}$  and a dispersion of  $19 \pm 4 \text{ km s}^{-1}$ . The uncertainties on these quantities have been estimated by boot-strap resampling of the datasets. Note that the velocity dispersions derived above are dominated by the large instrumental uncertainty in individual velocity measurements. To determine an upper limit on the velocity dispersions of the two populations, we performed further maximum-likelihood fits by including a Gaussian noise model for each datum (with  $\sigma$  equal to the cross-correlation uncertainties listed in Table 1). The resulting upper limit, at the 90% confidence level, is found to be  $17 \text{ km s}^{-1}$ , while that of the non-VRC population is  $18 \text{ km s}^{-1}$  (note that these values depend critically on whether the velocity uncertainties have been well estimated or not).

### 3. Discussion and summary

The heliocentric radial velocity of the H I at the center of gravity of the LMC has been found to be  $274 \pm 6 \text{ km s}^{-1}$  (Luks & Rohlfs 1992), while the velocity dispersion of the carbon stars that reside in the LMC disk is  $\sim 15 \text{ km s}^{-1}$  (Kunkel *et al.* 1997) independent of position. Evidently, the kinematic parameters of both our VRC and non-VRC samples are very similar to these values, supporting the hypothesis that the VRC is a stellar population of the LMC. However, the small velocity dispersion of the VRC population is also consistent with the expected velocity dispersion of Galactic tidal streams, judging from N-body disruption simulations of dwarf galaxies (see e.g. Ibata & Lewis 1998). Below, we use the small difference between the mean radial velocity of the LMC and the VRC populations to examine these two possible pictures.

The first possibility is that the VRC is a tidal stream that is unrelated to the LMC. We can obtain a rough estimate of how unlikely the observed coincidence of mean radial velocities is in this scenario, by assuming that the hypothesised tidal stream is a Galactic halo tracer (i.e. a random halo particle); if so, it must be drawn randomly from the halo distribution function. A reasonable model for the distribution function of the Galactic halo has been presented by Evans (1994). For the parameters of this “power law halo” model, we adopt those corresponding to the spherical Galactic halo model given in Evans & Jijina (1994). With these assumptions, and taking the mean velocity of our non-VRC sample as indicative of the mean velocity of the LMC in the observed field, we find that the probability that the difference in mean radial velocity between the LMC and the tidal stream should be as low as  $3 \pm 6 \text{ km s}^{-1}$  is very small,  $\sim 1\%$ . Note however, that the use of

the Evans & Jijina model in deriving this estimate probably exaggerates the unlikelihood of the observed velocity coincidence; most outer Galactic halo objects are known to be clustered on a great circle (see e.g. Lynden-Bell & Lynden-Bell 1995), so the two radial velocities in the above scenario are likely to be correlated.

Alternatively, the VRC could be a population of stars that is physically associated to the LMC. For instance, it is easy to imagine that some earlier galactic interaction (e.g. Zhao 1998b) could have ejected stars from the main body of the LMC, though without sufficient energy to unbind them. A further possibility is that the VRC are LMC halo stars, scattered between  $\sim 10$  kpc to  $\sim 25$  kpc in front of that galaxy. LMC halo objects should have a velocity dispersion approximately equal to the virial velocity dispersion of the system. Given the LMC mass of  $\sim 1.5 \times 10^9 M_\odot$  and half-mass radius  $\sim 7$  kpc (Kunkel *et al.* 1997), the virial velocity dispersion is  $\sim 60 \text{ km s}^{-1}$ , and the line-of-sight velocity dispersion is correspondingly a factor of  $1/\sqrt{3}$  smaller,  $\sim 35 \text{ km s}^{-1}$ . Thus it would appear that the coincidence between the systemic velocity of the LMC and that of the hypothesised stream should be unlikely; or alternatively, if the VRC is part of a diffuse halo population, it would appear that the velocity dispersion upper limit of  $17 \text{ km s}^{-1}$  is inconsistent with the expected dispersion. However, there will be a kinematic bias in our sample if either of these scenarios is correct. This effect is particularly pronounced due to the location of the ARGUS field on the sky, close to the dynamical center of the LMC. For instance, if the distribution function of the LMC halo has a substantial fraction of radial orbits, the fact that we have selected stars at large distances in front of the LMC means that we are also selecting stars close to turnaround, where they will preferentially have velocities close to the systemic velocity of their parent population. So the small velocity dispersion of the VRC and the small difference between the mean velocities of the VRC and the LMC cannot be used to discriminate against these models.

We have presented new kinematic data on a population of stars that has been seen in photometric studies of the center of the LMC. In the color-magnitude diagram, these stars extend vertically upwards from the well-known red clump. Being a rare phenomenon, Zaritsky and Lin (1997) hypothesised that this population belongs to a previously unknown stellar stream located  $\sim 20$  kpc in front of the LMC. The stellar components of the stream are extremely interesting due to their ability to bias LMC microlensing experiments. Strong doubts have already been cast on the arguments used by Zaritsky and Lin (1997) to reject a stellar evolution interpretation to this feature (Beaulieu & Sackett 1998), since simple stellar population modeling can reproduce from 75% to 100% of the observed densities. The radial velocity data presented in this contribution shows unambiguously that the “vertical red clump” population has identical kinematic properties to the LMC itself. If the VRC were a tidal stream, not associated to the LMC, the probability of this chance velocity

alignment appears to be quite small. However, our data do not discriminate against the possibility that the VRC is a stellar population gravitationally bound to the LMC. Whether this or another stellar population, perhaps a tidal streamer very close to the LMC (Zhao 1998a), is affecting the observed microlensing rate, still remains an open question.

This work was based on observations taken at the Cerro Tololo Inter-American Observatory, which is operated by AURA Inc. under contract to the National Science Foundation. We thank the anonymous referee for the pointing out the kinematic bias of our sample.

## REFERENCES

- Alcock, C. *et al.* 1998, ApJ 499, L9
- Alcock, C. *et al.* (The MACHO Collaboration) 1997a, ApJ 486, 697
- Alcock, C. *et al.* 1997b, ApJ 490, L59
- Beaulieu, J.-P. & Sackett, P. 1998, AJ 116, 209
- Bertelli, G., Bressan, A., Chiosi, C., Gaggotto, F. & Nasi, E. 1994, A&AS 106, 275
- Cook, K., 1998, in *The 4th international workshop on gravitational microlensing surveys*, Paris, Jan 15-17, 1998.
- Evans, N. W. 1994, MNRAS 267, 333
- Evans, N. W. & Jijina, J. 1994, MNRAS 267, L21
- Ibata, R. & Lewis, G. 1998, ApJ 500, 575
- Kunkel, W., Demers, S., Irwin, M. & Albert, L. 1997, ApJ 488, L129
- Luks, T. & Rohlfs, K. 1992, A&A 263, 41L
- Lynden-Bell, D. & Lynden-Bell, R. 1995, MNRAS 275, 429
- Sahu, K. 1994, Nature 370, 275
- Suntzeff, N., Mateo, M., Terndrup, D., Olszewski, E., Geisler, D. & Weller, W. 1993, ApJ, 418, 208
- Tonry, J. & Davis, M. 1979, AJ 84, 1511
- Zaritsky, D. & Lin, D.N.C. 1997, AJ 114, 2545 (ZL)
- Zhao, H.-S. 1998a, MNRAS 294, 139

Zhao, H.-S. 1998b, ApJ 500, 149

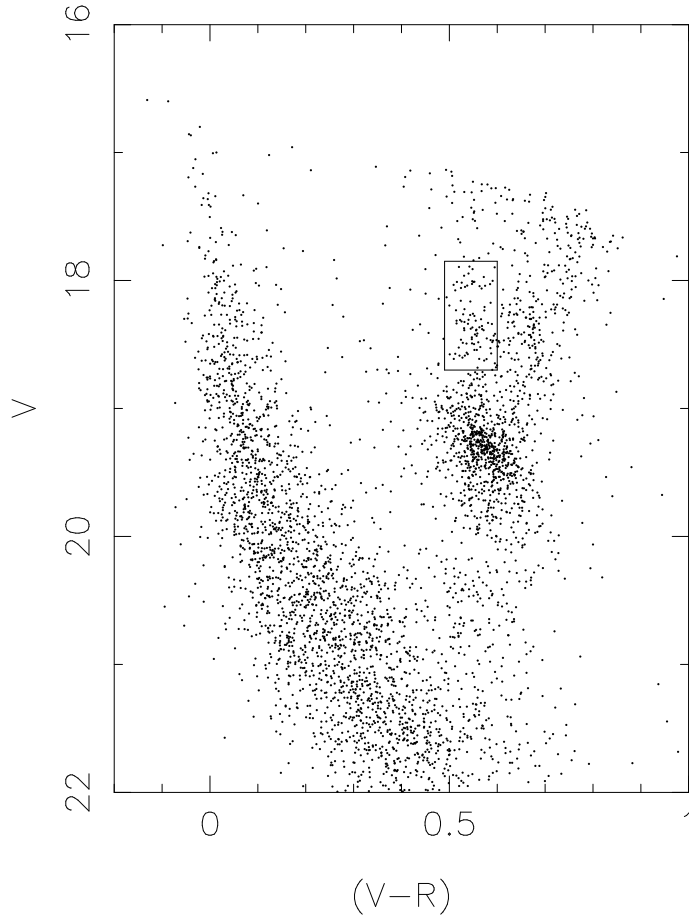


Fig. 1.— This color magnitude diagram shows a field at  $\alpha = 5^h 14'.7$ ,  $\delta = -68^\circ 49'.9$  (J2000), in the central regions of the LMC (Beaulieu & Sackett 1998). The “vertical red clump” (VRC) identified by Zaritsky and Lin (1997) is clearly seen within the boxed region in this diagram (the limits of this box were chosen by ourselves to encompass the population of interest).

Table 1. CTIO Radial Velocity Data

RA (2000)	DEC (2000)	V (mag)	V – R (mag)	$R_{TD}$	$V_{helio}$ (km/s)	$\Delta V_{helio}$ (km/s)	VRC member?
5 15 13.9	–68 45 4.24	17.14	0.21	17.68	234.	9.	n
5 15 4.3	–68 45 11.63	17.47	0.55	11.75	270.	14.	n
5 14 31.6	–68 45 15.08	18.07	0.42	5.88	273.	27.	n
5 14 53.5	–68 45 18.40	17.43	0.46	16.01	279.	10.	n
5 14 45.5	–68 45 20.07	17.72	0.37	8.39	253.	18.	n
5 14 59.6	–68 45 22.24	17.89	0.52	8.36	233.	19.	y
5 14 17.4	–68 45 33.64	18.48	0.59	16.33	251.	10.	y
5 14 36.3	–68 45 47.10	17.31	0.53	13.17	286.	13.	n
5 14 14.5	–68 46 3.30	17.14	0.42	10.97	263.	15.	n
5 14 23.2	–68 46 12.70	18.38	0.54	6.70	297.	21.	y
5 15 0.3	–68 46 17.27	18.04	0.57	14.41	255.	12.	y
5 14 49.9	–68 46 31.21	17.95	0.54	10.46	249.	17.	y
5 14 33.6	–68 46 39.44	18.01	0.55	10.49	256.	16.	y
5 15 8.5	–68 46 42.50	17.91	0.55	14.48	273.	11.	y
5 14 21.7	–68 46 50.10	18.47	0.60	6.65	266.	23.	y
5 14 15.7	–68 47 2.75	18.06	0.52	9.31	258.	17.	y
5 14 54.6	–68 47 10.47	18.23	0.57	7.85	253.	20.	y
5 14 22.5	–68 47 28.43	18.04	0.54	9.99	301.	16.	y
5 14 40.2	–68 47 35.13	17.18	0.51	21.43	267.	8.	n
5 15 8.9	–68 47 40.57	17.96	0.53	9.15	227.	18.	y
5 15 7.2	–68 47 41.18	18.16	0.54	6.03	250.	23.	y
5 14 21.7	–68 48 9.13	18.26	0.53	15.60	272.	11.	y
5 14 26.9	–68 48 9.55	17.98	0.26	5.07	249.	41.	n
5 15 12.0	–68 48 11.01	18.37	0.56	5.07	187.	37.	y
5 14 25.8	–68 48 41.62	17.31	0.55	20.27	263.	8.	n
5 15 11.6	–68 48 57.03	17.52	0.55	17.23	288.	9.	n
5 15 15.9	–68 48 57.21	17.16	0.46	14.76	265.	11.	n
5 14 16.2	–68 49 1.36	17.25	0.57	15.14	309.	11.	n
5 14 11.8	–68 49 16.10	17.54	0.52	14.66	273.	11.	n
5 15 0.0	–68 49 30.35	18.16	0.52	9.64	275.	19.	y
5 14 16.7	–68 49 37.67	18.23	0.51	6.11	280.	29.	y
5 14 38.9	–68 49 42.08	18.47	0.59	7.66	251.	20.	y
5 14 24.2	–68 49 46.84	18.28	0.55	10.03	287.	16.	y
5 14 55.8	–68 49 52.14	18.01	0.55	9.58	262.	17.	y
5 15 12.8	–68 49 55.98	18.47	0.60	25.19	260.	6.	y
5 14 14.4	–68 50 37.62	17.28	0.59	14.70	301.	11.	n
5 14 22.2	–68 50 37.71	17.50	0.53	23.26	252.	7.	n
5 14 21.3	–68 50 47.95	18.38	0.56	7.88	303.	25.	y
5 14 30.7	–68 50 57.88	18.48	0.56	5.86	299.	24.	y
5 15 12.3	–68 50 59.01	18.31	0.52	6.30	271.	20.	y



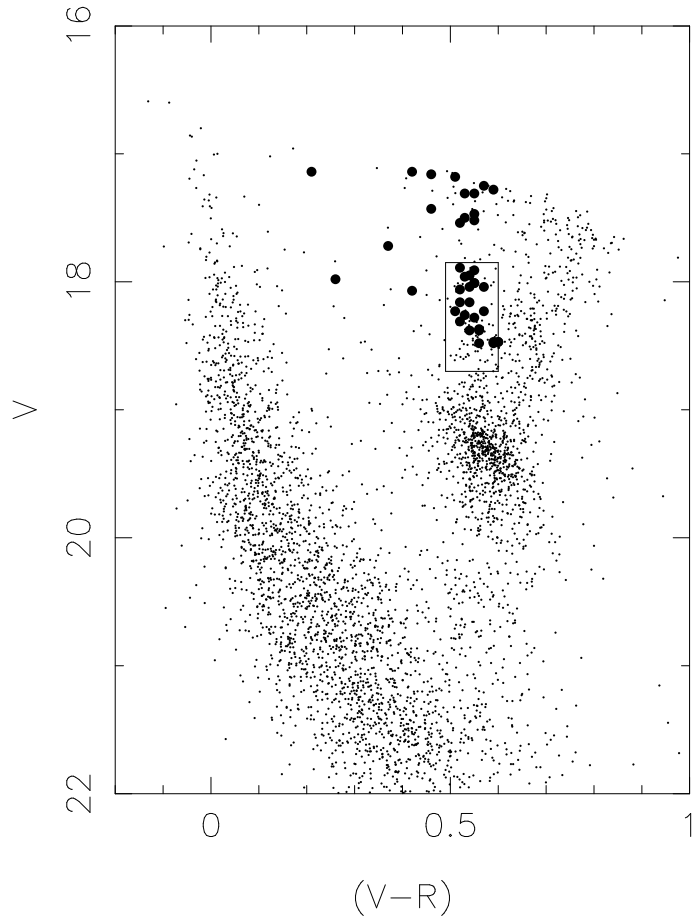


Fig. 2.— The color-magnitude positions of the spectroscopically observed stars are shown superimposed on the CMD of Figure 1. Of the 40 stars, 24 lie within the VRC box.

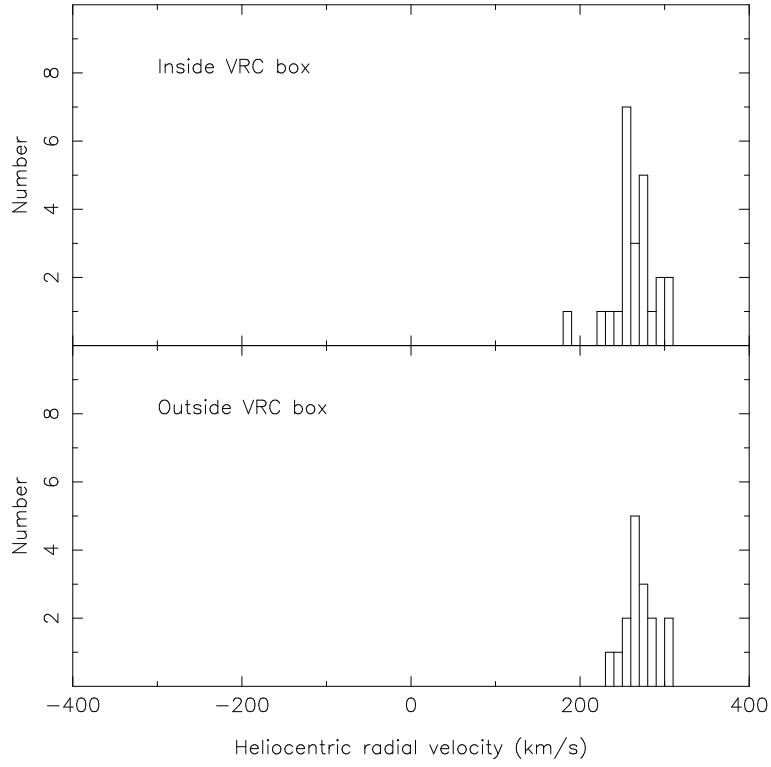


Fig. 3.— The top panel shows the heliocentric radial velocity distribution of the 24 stars that lie in the VRC box in Figure 2. The velocity distribution of all other stars is displayed in the bottom panel.